

85 Peg A: which age for a low metallicity solar like star?

F. D’Antona^{1*}, D. Cardini², M. P. Di Mauro³, C. Maceroni¹, I. Mazzitelli⁴
and J. Montalbán⁵

¹*INAF, Osservatorio Astronomico di Roma, via Frascati 33, I-00040 MontePorzio, Italy*

²*INAF, Istituto di Astrofisica Spaziale, via del Fosso del Cavaliere 100, I-00133 Roma, Italy*

³*INAF, Osservatorio Astrofisico di Catania, via S. Sofia 78, I-95123 Catania, Italy*

⁴*via Zambarelli 22, I-00044 Frascati, Italy*

⁵*Istitut d’Astrophysique et Géophysique Université de Liège, Allée du 6 Août, B-4000 Liège, Belgium*

18 October 2018

ABSTRACT

We explore the possible evolutionary status of the primary component of the binary 85 Pegasi, listed as a target for asteroseismic observations by the MOST satellite. In spite of the assessed ‘subdwarf’ status, and of the accurate distance determination from the Hipparcos data, the uncertainties in the metallicity and age, coupled with the uncertainty in the theoretical models, lead to a range of predictions on the oscillation frequency spectrum. Nevertheless, the determination of the ratio between the small separation in frequency modes, and the large separation as suggested by Roxburgh (2004), provides a very good measure of the star age, quite independent of the metallicity in the assumed uncertainty range. In this range, the constraint on the dynamical mass and the further constraint provided by the assumption that the maximum age is 14 Gyr limit the mass of 85 Peg A to the range from 0.75 to 0.82 M_{\odot} . This difference of a few hundredths of solar masses leads to well detectable differences both in the evolutionary stage (age) and in the asteroseismic properties. We show that the age determination which will be possible through the asteroseismic measurements for this star is independent either from the convection model adopted or from the microscopic metal diffusion. The latter conclusion is strengthened by the fact that, although metal diffusion is still described in an approximate way, recent observations suggest that the real stars suffer a smaller metal sedimentation with respect to the models.

Key words: Stars: binaries – Stars: asteroseismology – Stars: structure

1 INTRODUCTION

The bright visual binary 85 Peg (HD 224930) has been the object of numerous studies since the time of its discovery by Burham (1879). Spectroscopy revealed a metal deficient object and astrometry moderately high space velocity components (Allende Prieto et al. 2004; Nordström et al. 2004), both suggesting a classification as subdwarf and a probable old age. Its orbital elements are known with good approximation since a long time, and recent determinations, made through very precise astrometric, photometric and spectroscopic measurements (Griffin 2004, and references therein), have not substantially changed what has been known for more than one century nor have been able to solve the problem of the masses of the stars that constitute 85 Peg. Indeed, while it seems evident that, making the reasonable

hypothesis of a common origin, the secondary star should have a considerably smaller mass than the primary, due to the about three magnitudes of difference, the masses determined dynamically are similar. This discrepancy has been ascribed to a third much fainter component (Hall 1948). In this situation the determination of the two masses has been committed up to now to theoretical calibrations by modeling stellar parameters (Fernandes et al. 1998, Fernandes, Morel & Lebreton 2002) on the basis of observational data and of assumptions on age, initial helium content and metallicity. This leaves broad intervals of discreteness which, coupled with the uncertainty in the theoretical models, lead to rather different determinations of mass and consequently of age. The determination of the age of subdwarfs sets a lower limit to the age of old galactic stars, possibly significant as lower limit for the age of the Galaxy.

Recently, a new tool has become available to infer the evolutionary status and the structural properties of a star,

* E-mail: dantona@mporzio.astro.it

asteroseismology. During the last years, numerous attempts have been made with the aim of identifying oscillations in distant stars and also of modeling the stellar pulsational phenomena. It is now clear, indeed, that oscillations have several advantages over all the other observables: pulsational instability has been detected in stars in all the evolutionary stages and of different spectral type; frequencies of oscillations can be measured with high accuracy and depend in very simple way on the equilibrium structure of the model; different modes are spatially confined and probe different layers of the stellar interior.

85 Peg A can be considered as a good candidate for asteroseismic studies, since theory predicts a detectable surface amplitude of oscillations with a maximum value of $v_{\text{osc}} \simeq 18.8 \text{ cm s}^{-1}$ according to the scaling law of Kjeldsen & Bedding (1995) and a mean value of $v_{\text{osc}} \simeq 9 \text{ cm s}^{-1}$ (Houdek private communication) obtained according to the theoretical simulation of modes stochastically driven by convection (Houdek et al. 1999). 85 Peg A, indeed, is listed as target for asteroseismic observations by MOST (Walker et al. 2003), the first satellite totally dedicated to the observation of pulsating stars from space.

The aim of the present paper is to provide a comprehensive theoretical study of the system. We will use new theoretical evolution models to find a correspondence between the observed data and the derived astrophysical parameters, in order to locate 85 Peg A in an evolutionary context. We will discuss the possibility of discriminating among its possible structure models by means of the oscillation data which will be soon available.

A summary of known data on 85 Peg is presented in Section 2, the details of the evolutionary models and their result in Sections 3 – 5, the computations of the oscillation frequencies and a discussion of the results in Section 6 and 7, which is followed by the final conclusions.

2 A "THORN IN THE SIDE" OF EVOLUTIONARY THEORIES: THE VISUAL BINARY 85 PEGASI

The visual and single-lined spectroscopic binary 85 Peg is a bright ($V=5.75$), and nearby ($\sim 12 \text{ pc}$) system with an orbital period of 26.31 yr (Griffin 2004). Its small angular separation ($a = 0''.83$) and the marked magnitude difference between the components, $\Delta m \simeq 3.08 \pm 0.29 \text{ mag}$ in V (ten Brummelaar et al. 2000), makes it a difficult target both for visual and spectroscopic observations. The primary component is a metal deficient G5 subdwarf (Fulbright 2000), while the most-of-the-time unresolvable secondary is supposed to be, on the basis of the Δm value, a K6-K8 dwarf. The classification as subdwarf is based both on the space velocity component values and on its metallicity (Allende Prieto et al. 2004; Nordström et al. 2004, respectively $[\text{Fe}/\text{H}] = -0.88$ and -0.80). More recently Van’t Veer et al. (2005) found a smaller deficit, $[M/H] = -0.7$, which at any rate places it at least among old disk stars. According to Van’t Veer et al. (2005), the α -elements are enhanced by a factor ~ 2 with respect to solar scaled abundances.

An excellent summary and a critical analysis of the dynamical data, collected over more than a century, has been

Table 1. Orbital and astrometric parameters of 85 Peg

parameter	value	error	ref.
P (yr)	26.31	± 0.01	2
a	$0''.83$	$\pm 0''.01$	1
i	-49°	$\pm 1^\circ$	1
e	0.38	± 0.01	1
π (mas)	82.5	± 0.8	1
K_1 (km s^{-1})	4.49	± 0.05	2
γ (km s^{-1})	-36.22	± 0.03	2
$a_1 \sin i$ (AU)	3.68	± 0.04	2
$f(\mathcal{M})$ (\mathcal{M}_\odot)	0.0722	± 0.024	2

Reference coding: (1) Söderhjelm (1999), (2) Griffin (2004)

Table 2. Physical parameters of 85 Peg

parameter	primary	secondary	ref.
$\mathcal{M}/\mathcal{M}_\odot$	0.77 ± 0.05	0.72 ± 0.05	1
T_{eff} (K)	5600 ± 50	4200 ± 200	2,3
M_v	5.39 ± 0.04	8.47 ± 0.29	4
L/L_\odot	0.617 ± 0.02	0.072 ± 0.03	4
$[M/H]$	-0.7 ± 0.1		2
$\log g$	4.6 ± 0.1		2

Errors are standard deviations. Reference coding: (1) Griffin (2004), (2) Van’t Veer et al. (2005), (3) Fernandes et al. (2002) (4) present paper

recently published by Griffin (2004) together with a long term radial velocity study, therefore we report here only the strictly necessary information and refer to the quoted paper for a more complete review. The main updated orbital parameters from various sources are collected in Table 1.

The often quoted (Lippincott 1981; Griffin 2004) remark by Struve (1955) on 85 Peg: “this double star is a thorn in the side of the present evolutionary theories of single stars and of widely separated double stars” essentially refers to the discrepancy between the reduced mass ($B = \mathcal{M}_2/(\mathcal{M}_1 + \mathcal{M}_2)$), as derived from astrometry, and the value expected on the basis of the magnitude difference. The former is typically around 1/2, e.g. the recent value $B = 0.528 \pm 0.034$ from Hipparcos results (Martin & Mignard 1998), and implies a secondary star equally or slightly more massive than the primary, the latter is around $B = 0.38$. With a well constrained total mass of $\mathcal{M} = 1.49 \pm 0.1 \mathcal{M}_\odot$ the secondary mass varies, then, from 0.77 to $0.55 \mathcal{M}_\odot$.

The value of the reduced mass from astrometry is confirmed by the spectroscopic orbit of Griffin (2004), as his value of the mass function $f(\mathcal{M}) = 0.0722 \mathcal{M}_\odot$, when coupled to the total mass and inclination from visual observations, provides $B = 0.482 \pm 0.019$, in good agreement with the abovementioned value. A possible and straightforward explanation is that the secondary is in its turn a binary system, with an undetected secondary (85 Peg Bb) storing the “excess” mass (a few tenths of solar mass). This hypothesis was already put forward by Hall (1948) and reappears in a number of subsequent works.

The atmospheric parameters of 85 Peg have been as well the subject of several studies. An accurate determination of the primary effective temperature and chemical

composition, by fitting of the Balmer line wings, was obtained by Van't Veer (2000), as reported in Fernandes et al. (2002, hereafter FML02), and has recently been updated (Van't Veer et al. 2005). According to the latter work, the primary effective temperature is $T_{\text{eff}} = 5600 \pm 50$ K. Other, somewhat different, determinations yield also lower values; Fulbright (2000) obtained the lowest one ($T_{\text{eff}} = 5275$ K), but the discrepancy is presumably due to the derivation of the temperature from the FeI lines under the assumption of LTE. Thévenin & Idiart (1999) showed that non-LTE effects can affect the result in the case of sub-dwarfs and the same Fulbright (2000) finds indeed a systematic effect, his temperatures being lower than those from other methods.

The individual absolute magnitudes and relative errors were determined by us using the apparent magnitudes and relative errors given by ten Brummelaar et al. (2000) who got *BVRI* differential photometry of the components by means of adaptive optics, and derived the individual magnitudes from these and from the composite magnitudes found in Mermilliod, Mermilliod & Hauck (1997). We used, moreover, the Hipparcos parallax and errors as corrected by Söderhjelm (1999) for binarity effects. The bolometric corrections were obtained from the best fit coefficients of Flower (1996). The physical parameters of the binary are collected in Table 2. Errors on luminosities do not take into account the uncertainty on bolometric correction which should be negligible at the primary temperature but could be relevant for the secondary component.

FML02 determined by a least square algorithm the set of physical parameters, with their evolutionary stellar code, that best fit the available photometric, astrometric and spectroscopic data (under the hypothesis of equal age and chemical composition of the components). They used, however, as input to the procedure, a rather lower value for the reduced mass ($B = 0.44$ vs. $B = 0.482$ from Griffin 2004). Consequently they determine a value for the primary mass, $0.88 M_{\odot}$, which is significantly larger than Griffin's one. These authors derive a best fit age of 9.3 ± 0.5 Gyr and a (today's) metallicity value $[\text{Fe}/\text{H}] = -0.55$.

3 MODELING

We use the Aton 3.0 version of the Aton code (Mazzitelli 1979) whose main physical inputs are described in Ventura & D'Antona (2005). We describe here the properties of this version of the code which are relevant to the computation of the oscillation frequencies: namely the choice of opacities, the modeling of convection and diffusion, and the computation of an updated equation of state. Only models having gray boundary conditions are used in this work.

3.1 Opacities

We adopt the Alexander & Ferguson (1994) opacities at temperatures smaller than 12000 K, and the OPAL opacities, in the version documented by Iglesias & Rogers (1996). Opacities and thermodynamics are computed in the code according to the prescriptions given in the following Section.

3.2 Equation of state

Tables of equation of state (EOS) are computed outside the main code. For each metal abundance, represented by the mass fraction Z , six tables are built, with hydrogen content X from 0 to $1-Z$. The input variables are temperature T and gas pressure P_{gas} , and the output quantities are the density ρ , specific heat at constant pressure C_p , the ratio $\gamma = C_p/C_v$, the adiabatic gradient ∇_{ad} , χ_{ρ} and the exponents Γ_1, Γ_2 and Γ_3 . Simple functional relations then provide any other thermodynamic quantity. Tables are rectangular in the plane T - P_{gas} , in order to simplify interpolation by means of third degree bidimensional spline functions. Notice that the regions of very high temperature and very low pressure are never used, and are filled up with simple formulations of the EOS, only to provide more convenient interpolation. The tables are filled up in three steps: first the thermodynamic quantities are computed according to the formulation by Stolzmann & Blöcker (1996, 2000) for fully ionized gas. This EOS allows to consider explicitly different elements mixtured. It includes degeneracy (both classic and relativistic), coulombian effects, exchange interactions and other corrections, and it is the most modern description available for ionized gas. It holds, however, only for high densities.

The region in which pressure ionization is important is overwritten with Saumon, Chabrier, & van Horn (1995) EOS. In this way we fill the whole region in which the gas is not ionized. However, Saumon, Chabrier, & van Horn (1995) EOS is only given for pure hydrogen and pure helium, without metals. Therefore the metallicity Z is "simulated" through Y and the different hydrogen - helium mixtures are interpolated through the additive volume law. This is particularly unsafe where strong configurational effects are expected, and the interpolation error may amount to $\sim 20\%$ for normal H-rich mixtures (Montalbán et al. 2000).

Use of Saumon, Chabrier, & van Horn (1995) EOS is limited to a small region of the T - P_{gas} plane, by overwriting it with the OPAL 2001¹ EOS (Rogers, Swenson, & Iglesias 1996; Rogers 2001), which is given for any Z and ratio H/He. This EOS extends also to low pressures.

After these large tables are written, for a given Z , six values of each physical quantities are computed for 6 different Y . A cubic unidimensional spline provides the interpolation for any input value of Y . The six tables for H/He and given Z are supplemented by fifteen tables He/C/O in which the EOS is directly computed according to Stolzmann & Blöcker (1996) as the non ionized regions are not present in stellar structure following helium ignition. The interpolation among the fifteen tables is done by triangles in the plane C/O, as the stochiometric condition is $Y=1-X_C-X_O$.

In summary, the structure code computes the EOS quantities and the opacities memorizing the spline coefficients, and this allows to obtain full continuity both in the physical quantities and their first and second derivatives, a feature important when we deal with the computation of multi-mode pulsations.

¹ the WEB version dated March 2002 is used

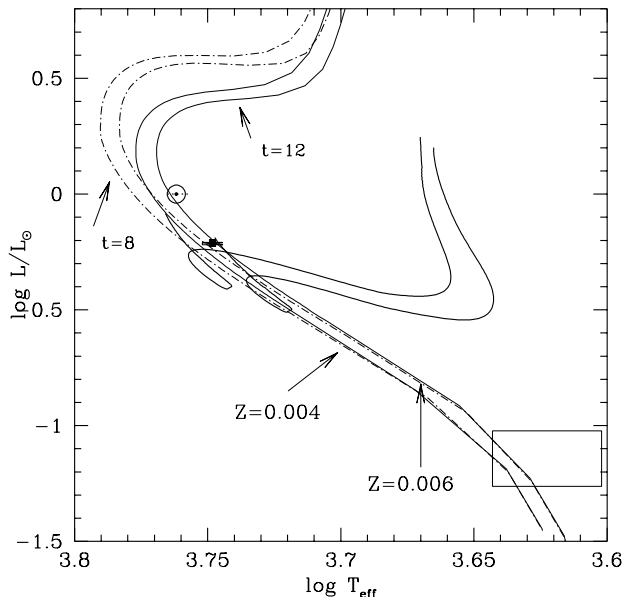


Figure 1. The location of 85 Peg A (full dot with the small error box) and 85 Peg B (box) in the HR diagram, according to the data in Table 2. The present solar location is also shown. We plot isochrones of $t=8$ (dash-dotted) and 12 Gyr (dotted) lines for metallicities $Z=0.004$ and $Z=0.006$. For both sets of models $Y=0.24$. Two evolutionary tracks are also shown (solid lines), which bracket the reasonable range of ages for the star: $0.791 M_{\odot}$ ($Z=0.004$), which has an age of about 8 Gyr at the luminosity of 85 Peg A (model 4), and $0.775 M_{\odot}$ ($Z=0.006$), age $t \simeq 14$ Gyr (model 5).

3.3 Diffusion

The code includes both gravitational and thermal helium diffusion according to Iben & McDonald (1985). Helium diffusion is a key ingredient in the solar model, necessary to adequately reproduce the run of the sound speed as derived from the extremely precise helioseismological data (Basu, Pinsonneault & Bahcall 2000).

3.4 Convection

Convection in the code can be treated either according to the Full Spectrum Turbulence (FST) model by Canuto & Mazzitelli (1991) and Canuto, Goldman & Mazzitelli (1996), or according to the classic mixing length theory (MLT) model (Böhm-Vitense 1958). A detailed description of the convective model is given in Ventura et al. (1998). The FST model is characterized by convective fluxes in which the full eddies distribution is accounted for, and by a convective scale length defined as the harmonic mean between the distance of the layer from the top and the bottom of the convective zone. In addition, the distance to the top (and bottom) is increased by a fraction βH_p , where β is calibrated in order to obtain the observed solar radius at the solar age (in the range $\beta = 0.1 - 0.2$). Non instantaneous mixing is generally used as described by Ventura et al. (1998). The mixing is treated as a diffusion, with the diffusion velocity obtained

in the framework of the FST model. This mixing is very relevant for hydrogen or helium burning in convective cores, but it is not strictly important in this work, as we will be dealing only with burning of hydrogen in radiative cores.

3.5 Numerical resolution

Particularly to compute the solar structure to be compared with the very precise results of helioseismology, we take care to have a very good numerical resolution of the structure, both in the temporal evolution (about 1000 time-steps are taken to reach the solar age) and spatial resolution (about 2000 mesh points are adopted). For the exploratory models relative to 85 Peg A presented in this work, we only employ ~ 800 mesh points and broader temporal evolution. In any case we took care of having an appropriate distribution of meshes both in the central region (to have a careful computation of nuclear evolution), in the overadiabatic region and close to the bottom of the external convective region (to have a careful computation of the oscillation frequencies).

3.6 Use of solar-scaled abundances

In the code, we did not yet implement the use of α -enhanced opacities and EOS. At present, the uncertainties both in the metallicity determination and in the metal diffusion (see next section) are such that this improvement is not yet necessary, although it must be planned for the future. For population II stars, we follow the suggestion by Salaris et al. (1993), who have shown that the effect of the increase of α -elements abundances in the energy production and opacities can be mimicked by increasing the total metal abundance.

4 METAL DIFFUSION IN PRESENT EVOLUTIONARY CODES

The current version of the evolutionary code does not include metal diffusion, whose effect is however much controversial. In fact, the same “*sign*” of metal diffusion is not yet clear, particularly in the context of low metallicity stars. The problem is widely discussed by Gratton, Sneden & Carretta (2004). First of all, the theoretical results differ according to the description employed: most results based on the description by Thoul, Bahcall, & Loeb (1994), which is widely used, predict for the metallicity of the cluster NGC 6397 a depletion in $[\text{Fe}/\text{H}]$ by 0.2 – 0.4 dex (depending on the age) at the turnoff. On the other hand, the recent models by Richard et al. (2002), that take into account the effect of partial ionization and radiative accelerations, show that whereas some elements like He and Li are expected to be depleted, others (like Fe) are expected to be significantly enhanced. From the observational point of view, Gratton et al. (2001) find that turnoff and subgiant stars in the globular cluster NGC 6397 have the same metal abundance within 0.1 dex. This is neither consistent with models which predict a strong diffusion in main sequence, nor with Richard et al. (2002) models, as there should be a large difference between the turnoff abundance –where the metals have been either partially depleted from the whole convective region, or enhanced– and the subgiants, where deep convection should have restored the initial metallicity.

In any case, standard models predict that the effect of diffusion at the turnoff of globular cluster stars increases when decreasing the metallicity, as the main sequence shifts to increasingly hotter temperatures, for which the external convective layers are smaller, providing higher diffusion velocities at their bottom. Therefore, a negligible metal diffusion is expected for 85 Peg A, in view of the very small –if any– effect present in the much more metal poor cluster NGC 6397.

In view of these results, it is difficult to accept such a large effect as produced in the models by FML02, which start with a quasi-solar metallicity ($[\text{Fe}/\text{H}] = -0.185$) to arrive at the present metallicity, assumed to be $[\text{Fe}/\text{H}] = -0.55$. In particular, these models would require that the high velocity giants in Hipparcos catalogue have on average metallicities larger by a factor two than their turnoff or main sequence counterparts, a feature which has not been observed.

Nevertheless, in order to quantify the effect of the metal diffusion, we have also considered models computed by employing the Code Liégeois d'Évolution Stellaire (CLES) in which the helium and metal diffusion has been implemented according to Thoul et al. (1994). Comparisons between models calculated with and without metal diffusion will be shown in Sec. 7.2.

5 85 PEG IN THE EVOLUTIONARY CONTEXT

We computed, by using the Aton code, two sets of evolutionary tracks for 85 Peg A and B with helium mass fraction $Y = 0.24$ and metal mass fraction $Z=0.004$ and $Z=0.006$ corresponding, respectively, to solar scaled abundance $[\text{Fe}/\text{H}] \sim -0.70$ (Van't Veer et al. 2005) and $[\text{Fe}/\text{H}] \sim -0.55$ (FML02). Considering these two different metallicities, we also get a first understanding of the uncertainty due to the adoption of solar scaled abundances in our code. The cross section are computed according to the NACRE compilation (Angulo et al. 1999). All the models apart from model 9 in Table 3 adopt the FST treatment of the convective transport of energy in the interior, with a fine tuning parameter $\beta = 0.17$. In order to quantify the effect of the treatment of convection on the pulsational properties of the star, we also computed a track using the Böhm–Vitense mixing length formalism (MLT) with $\alpha_{MLT} = l/H_p = 1.7$ (model 9). The α value has been chosen so that the MLT and FST tracks have the same location in the HR diagram.

According to its space velocity, 85 Peg belongs to a group of moderate - high velocity stars, whose age is statistically limited to be larger than ~ 8 Gyr (Caloi et al. 1999). We have then considered $8 \lesssim t \lesssim 14$ Gyr as possible ages for 85 Peg. In Table 3 are collected, for each Z , the mass of the model reaching the luminosity observed for 85 Peg A (see Table 2) at the assumed ages of about 8, 10, 12 and 14 Gyr. Fig. 1 shows the locations of 85 Peg A and B according to the data from Table 2, the 8 and 12 Gyr isochrones for the different metallicities and two extreme evolutionary tracks (model 4 and 5). We notice that all the computed isochrones are compatible with the location of 85 Peg B. The 12 Gyr isochrones of both metallicities are consistent with the T_{eff} location of 85 Peg A, while the isochrone of $Z=0.004$ and $t = 8$ Gyr has a too large T_{eff} . However, we can consider

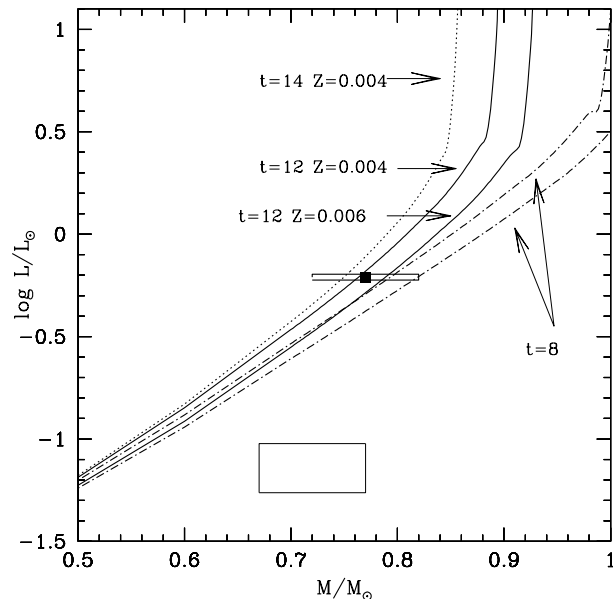


Figure 2. The masses and luminosities of 85 Peg A and 85 Peg B, as derived by Griffin (2004), are compared with the mass luminosity relation of the computed isochrones shown in Fig. 1 and with that for $t=14$ Gyr and $Z=0.004$ [model 1]. If one excludes ages larger than ~ 14 Gyr, the minimum acceptable mass is $\sim 0.75 M_{\odot}$.

as well this last isochrone on the basis of uncertainties on temperature. On the observational side, the error of only ± 50 K assigned to the T_{eff} determination certainly does not include consideration of possible systematic errors. From the stellar structure modeling side, we do know that precise T_{eff} 's can not be obtained from first principles. In particular, we employ grey atmosphere models: Montalbán et al. (2001) have shown that non gray models for low metallicity predict slightly lower T_{eff} than gray models (by ~ 80 K at $Z=0.0002$). Our results adopt the FST convection model, but a convective model with a slightly smaller efficiency may provide smaller T_{eff} . In summary, the models for $Z=0.004$ (the best value for the metallicity determined from spectra) and ages smaller than 12 Gyr have also full right to be considered in relation to 85 Peg, as we will check by looking at the mass luminosity relation.

The mass luminosity relation provides a better information than the HR diagram, as it is not affected by the uncertainty in T_{eff} . The mass luminosity relations of the computed isochrones shown in Fig. 1 are given in Fig. 2 with also that for $t \simeq 14$ Gyr and $Z=0.004$. The location of 85 Peg A according to the data in Table 2, taking into account the uncertainties, is in good agreement with all the computed $Z=0.004$ or $Z=0.006$ isochrones. Besides, in the hypothesis of an age smaller than 14 Gyr, we can put a lower limit to the primary mass at $0.75 M_{\odot}$. In summary, we can consider for our analysis all the models at the luminosity of 85 Peg A, from $0.75 M_{\odot}$ ($Z=0.004$), which has an age of ~ 14 Gyr to $0.82 M_{\odot}$ ($Z=0.006$) which has an age of ~ 8 Gyr.

Notice the location of 85 Peg B in the figure: indeed its dynamical mass is much larger than any acceptable value

Table 3. Selected models for 85 Peg A

mod.	convection	$\mathcal{M}/\mathcal{M}_\odot$	Z	t(Gyr)	L/L $_\odot$	R/R $_\odot$	T $_{\text{eff}}$	X $_c$
1	FST	0.750	0.004	13.80	0.616	0.817	5661	0.1670
2	FST	0.763	0.004	11.96	0.617	0.810	5689	0.2103
3	FST	0.778	0.004	9.97	0.619	0.803	5716	0.2669
4	FST	0.791	0.004	8.31	0.618	0.797	5737	0.3240
5	FST	0.775	0.006	13.97	0.619	0.846	5572	0.1653
6	FST	0.788	0.006	12.10	0.618	0.841	5587	0.2100
7	FST	0.803	0.006	10.08	0.618	0.833	5615	0.2675
8	FST	0.820	0.006	7.88	0.616	0.823	5644	0.3443
9	MLT	0.803	0.006	10.02	0.615	0.833	5608	0.2706

at that given luminosity. If we consider the value given by Griffin (2004), the dynamical mass of the secondary component is $\sim 0.2 \mathcal{M}_\odot$ larger than the possible main sequence mass. In the hypothesis that 85 Peg B is in its turn a binary system, its primary component, 85 Peg Ba, should have a mass of $\approx 0.52 \mathcal{M}_\odot$ (depending on the age), and its companion, 85 Peg Bb, of about $0.2 \mathcal{M}_\odot$. Accordingly, the luminosity of component Bb would be $\approx 0.0085 L_\odot$ and that of the primary of $0.064 L_\odot$ (as the value in Table 2 would refer to the composite luminosity). The binary nature of 85 Peg B could be checked by spectroscopic or interferometric observations (depending on its unknown period), if an instrument capable of separating the components of the visual binary is used, such as an adaptive optics telescope. The various possibilities in relation to the expected orbital period have already been examined in Griffin (2004).

In the next Sections the models are taken as input to derive the oscillation spectrum.

6 PULSATION ANALYSIS

We use the adiabatic oscillation code by Jørgen Christensen-Dalsgaard available in the WEB to calculate the p-mode eigenfrequencies. Some analytical and numerical aspects of oscillation codes are described in Christensen-Dalsgaard and Berthomieu (1991).

From the asteroseismic point of view 85 Peg A can be classified as a solar-type star, a main-sequence star in which oscillations are excited stochastically by vigorous near-surface convection in a broad spectrum of low amplitude p-modes, as in the Sun. The interpretation of the pulsational properties of a solar-type star can be obtained by considering the asymptotic theory (Tassoul 1980). This predicts that the oscillation frequencies ν_{nl} of acoustic modes, characterized by radial order n at harmonic degree l , should satisfy the following approximation:

$$\nu_{nl} = \Delta \left(n + \frac{l}{2} + \alpha + \frac{1}{4} \right) + \epsilon_{nl}, \quad (1)$$

where α is a function of the frequency determined by the properties of the surface layers and ϵ_{nl} is a small correction which depends on the conditions in the stellar core. Δ is the inverse of the sound travel time across the stellar diameter:

$$\Delta = \left(2 \int_0^R \frac{dr}{c} \right)^{-1}, \quad (2)$$

where c is the local speed of sound at radius r and R is

the photospheric stellar radius. The property expressed by Eq. (1) may provide almost immediate asteroseismic inferences on stellar parameters and constraints on theoretical models for a variety of solar-like stars in a wide range of evolutionary stages. For a given l , the acoustic spectra show a series of equally spaced peaks between p modes of same degree and adjacent n , whose frequency separation represents the so called large separation which is approximately equivalent to Δ :

$$\Delta \simeq \nu_{n+1l} - \nu_{nl} \equiv \Delta_l. \quad (3)$$

The spectra are characterized by another series of peaks, whose narrow separation is d_{ll+2} , known as small separation:

$$d_{ll+2} \equiv \nu_{nl} - \nu_{n-1l+2} = (4l+6)D_0 \quad (4)$$

where

$$D_0 = -\frac{\Delta}{4\pi^2\nu_{nl}} \left[\frac{c(R)}{R} - \int_0^R \frac{dc}{dr} \frac{dr}{r} \right]. \quad (5)$$

Δ , and hence the general spectrum of acoustic modes, scales approximately as the square root of the mean density, that is, $\Delta \propto \sqrt{\bar{\rho}} = \sqrt{\mathcal{M}/R^3}$. On the other hand, the small frequency separations are sensitive to the chemical composition gradient in central regions of the star and, hence, to its evolutionary state. Thus, the determination of both large and small frequency separation, Δ_l and d_{ll+2} , provides measures of the mass and of the age of the star (e. g. Christensen-Dalsgaard 1988).

6.1 Sub-surface effects and the ratio of small to large separation

The seismic analysis of observed acoustic frequencies is an extremely powerful tool for the investigation of the internal structure of the stars, but the use of large and small separations can be misleading if not accurately considered. Theoretical pulsation frequencies, essential for asteroseismic investigation, are calculated on theoretical models of stars which are inevitably affected by errors. In particular, the structure of the near-surface regions of stars, which strongly affects the large separation, is quite uncertain. In fact, there are still substantial ambiguities in the theoretical description of: i) the convective flux, ii) the mechanisms of excitation and damping of the oscillations, iii) the equation of state to describe the thermodynamic properties of the stellar structure, and iv) the non-adiabatic effects. Limiting the

investigation to the use of small separation does not solve the problem, since the small separation, which is determined principally by the conditions in the core, also retains some sensitivity to the mean density and to the detailed properties of the stellar envelope.

To solve these problems, the use of a new seismic indicator was introduced by Roxburgh & Vorontsov (2003), who compared the pulsating properties of several models with exactly the same interior structure, but with different outer envelopes. They showed that the ratios of small to large separations,

$$r_l = d_{l+2}/\Delta_l, \quad (6)$$

are independent of the structure of the outer layers and, hence, can be used as diagnostic of the interior of stars.

6.2 Echelle diagram

In order to study the large and small separations of the observed and computed oscillation frequency spectra, it is common to use the *echelle diagram* (Grec, Fossat & Pomerantz 1983). In this diagram each frequency is expressed in terms of an integer multiple of Δ , according to

$$\nu_{nl} = \nu_0 + k\Delta + \tilde{\nu}_{nl}, \quad (7)$$

where ν_0 is an arbitrary reference frequency, k is an integer and $\tilde{\nu}_{nl}$ is a residual frequency which lies in the range $0 - \Delta$. Plotting $\nu_0 + k\Delta$ against $\tilde{\nu}_{nl}$ one expects, according to the asymptotic theory (Eq. 1), that computed frequencies fall in parallel columns, one for each harmonic degree. The distance between consecutive frequencies of same harmonic degree, belonging to the same column, represents the large separation; modes of even degree (0 and 2) and modes of odd degree (1 and 3) fall in two pairs of closely spaced columns, the distance between the columns in each pair representing the small separation.

7 PREDICTION OF THE OSCILLATION FREQUENCIES OF 85 PEG A

We computed eigenfrequencies for all the selected structure models described in Table 3 and consistent with the observed basic parameters of the primary component of 85 Peg. Since the oscillation modes which can be detected in stars are generally characterized by low harmonic degree (owing to the point-like character of the sources), we limited our analysis to the calculation of modes with harmonic degrees $l = 0, 1, 2, 3$. Theoretical calculations on the selected models predict that 85 Peg A is pervaded by acoustic modes with frequencies in the range $1000 - 5000 \mu\text{Hz}$ for harmonic degrees $l = 0 - 3$. The oscillation spectrum is characterized by a large separation for the radial modes Δ_0 of about $150 - 170 \mu\text{Hz}$ (Fig. 3).

As predicted by theory, the value of the large separation decreases as the mean density decreases. For fixed metallicity, the large separation increases with the mass. In fact, the large separation strongly depends on the condition on the surface, and hence on the value of the metallicity. This means that the value of the mass cannot be estimated from the observed large separation alone.

It is very instructive to consider the behaviour of the

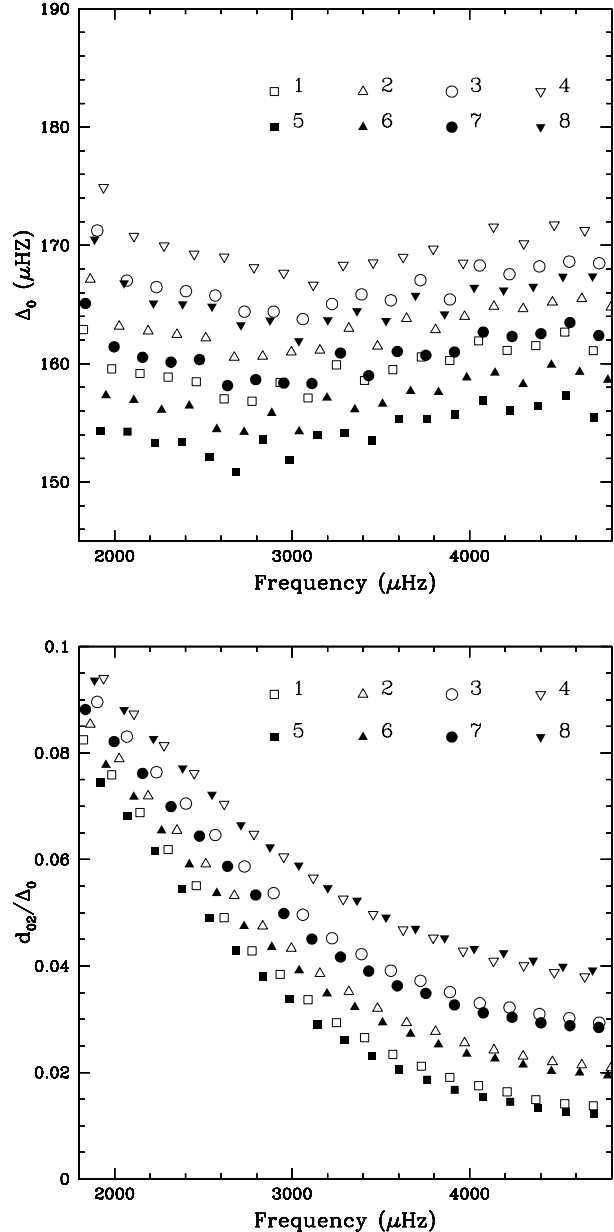


Figure 3. Open symbols refer to models with $Z=0.004$, filled symbols to $Z=0.006$, equal symbols correspond to models of similar age. Upper figure: large separation Δ_0 for $l = 0$ as function of the frequency calculated for selected models described in Table 3. Lower panel: ratio of small d_{02} to large separations Δ_0 between $l = 0$ and $l = 2$ for eight models of Table 3.

large separation as a function of frequency (Fig. 3). Consistently with the solar case, the theoretical Δ_l shows an evident oscillatory dependence on frequency. Such quasi-periodic behaviour of the frequencies rises from discontinuity's regions localized at certain acoustic depth in the structure. This peculiar property of the oscillation frequencies can be used to infer the helium abundance in the stellar envelope or to determine the properties and the location of the base of the convective envelope (e.g. Basu et al. 2004; Mazumdar & Antia 2001; Monteiro & Thompson 1998;

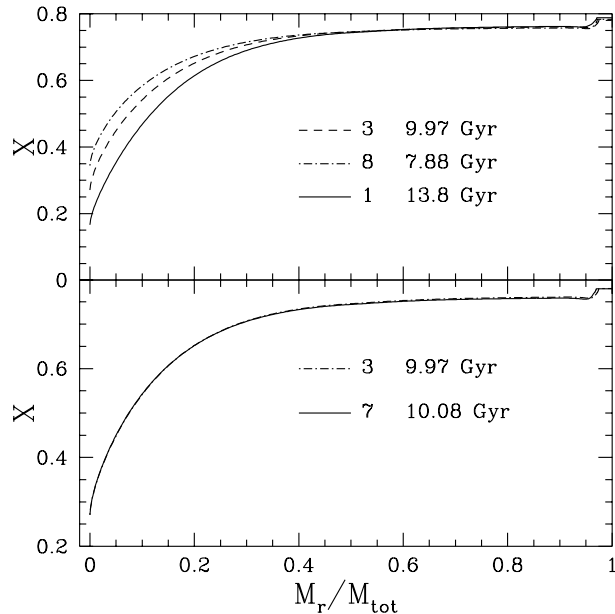


Figure 4. The top figure shows the hydrogen mass fraction X along the structure of selected models for increasing age. The bottom figure shows that the two models having age close to 10 Gyr have an almost equal hydrogen profile in spite of the different metallicity.

Monteiro, Christensen-Dalsgaard & Thompson 1994, 1998, 2000, 2002).

Fig. 3 employs the parameter $r_0 = d_{02}/\Delta_0$ devised by Roxburgh & Vorontsov (2003), in order to subtract the contribution of the surface layers, yielding a diagnostic of the stellar interior alone. In fact, the difference in d_{02}/Δ_0 among the models is easily understood in terms of the different internal structure: independently of the metallicity of the models, it is the core hydrogen content –and thus the age reached at the luminosity of 85 Peg A– which determines d_{02}/Δ_0 . Thus, models in the same evolutive state have the same value of r_l . The plot of hydrogen mass fraction X inside some of the examined structures is shown in Fig. 4.

It is clear that while measurements of small separation (or ratio r_l) will be useful to define the evolutive state of the star, the large separation will be employed to identify, among structures of same age, elements abundances and mass of the model which better reproduces the observations.

7.1 MLT versus FST models

While we adopt the FST model as a standard for the overadiabatic convection, we have made a comparison between model 7, computed with FST, and model 9, computed with the MLT. We adopt $\alpha = l/H_p = 1.7$, which provides a track having the same T_{eff} location of the FST track. The comparison is made in Fig. 5: there is a difference of about $1\mu\text{Hz}$ in the large separations for $l = 0$, while the ratios r_0 of the two models are very similar. Thus we conclude that the convection treatment does not affect the age determination by the seismic analysis.

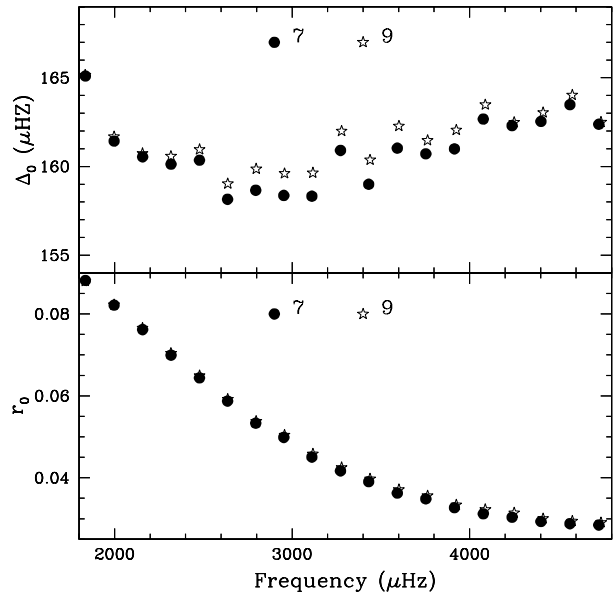


Figure 5. Large separation Δ_0 for $l = 0$ (top figure) and ratio of small to large separation (bottom) for model 7 and 9 of Table 3, having same mass and radius and nearly the same age of 10 Gyr. The models differ in the modelling of the external convective layers: FST for model 7 and MLT for model 9.

7.2 The metal diffusion

The ATON code does not include metal diffusion, so we adopt an entirely different code to have an idea of the influence of this physical input on the structure. The stellar structure and evolution code CLES adopts OPAL 2001 EOS; OPAL96 opacity tables plus Alexander & Ferguson (1994) at $T < 6000$ K; nuclear reaction rates from Caughlan & Fowler (1988); MLT convection treatment; atmospheric boundary conditions given by Kurucz (1998) at $T = T_{\text{eff}}$. Microscopic diffusion of all the elements is computed by using the subroutine by Thoul et al. (1994). A detailed comparison of the results of the CLES and ATON codes is out of the purpose of this paper, although it is in our research projects. We list in Table 4 the physical parameters of two models in the error box of 85 Peg A. We choose a large age (12 Gyr) to make the comparison, in order to maximize the effect of diffusion. The initial metallicity is $Z=0.006$, corresponding to $[Z/X]_0 = -0.555$. Model 11 includes only helium diffusion², while model 10 includes both helium and metal diffusion. At the age of 12 Gyr $[Z/X]_s$, the value at the surface of model 10 has been reduced by $\sim 33\%$ ³, a relatively mild effect which

² Notice that the CLES model has $X_c = 0.20$ in the center, while the corresponding ATON model 6 has $X_c = 0.21$, in spite of being slightly older. The treatment of helium diffusion differs in the two codes. The description in the ATON code (Iben & McDonald 1985) provides smaller diffusion velocities and this leads to this difference in X_c after 12 Gyr.

³ Notice that this decrease in $[Z/X]_s$ in the surface layers is due both to the decrease in Z and to the increase of X due to the helium diffusion (this can be seen, e.g. in Fig. 5 and from the change of $[Z/X]_s$ also in model 11 which has constant Z).

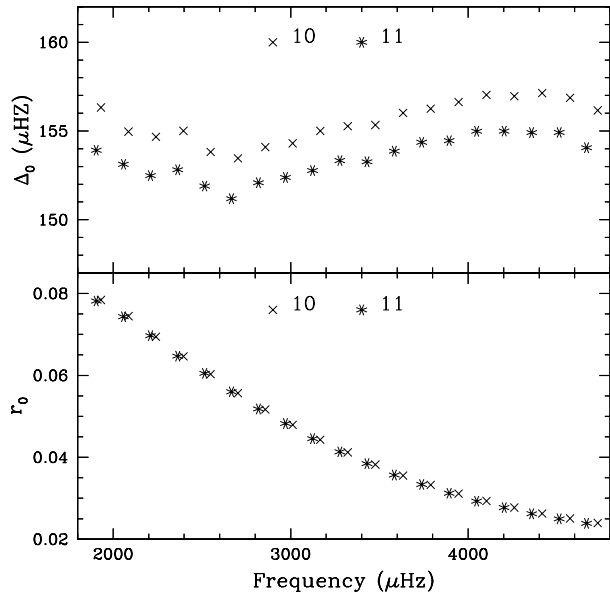


Figure 6. Comparison between the CLES models showing the effect of metal diffusion on the large separation (top) and on the ratio of small to large separation (bottom).

confirms the prediction made in Section 4 that metal diffusion on a star having the T_{eff} of 85 Peg A should not be dramatic. We show in Fig. 6 the oscillation properties of two models. We can see that the large separations differ by $\sim 2\mu\text{Hz}$, but the ratio r_0 is again very similar. Thus we conclude that the uncertainty in the computation of metal diffusion in the case of 85 Peg A is totally contained into the uncertainty in metallicity, and does not affect the age determination.

7.3 Echelle diagrams

In Fig. 7 we compare the echelle diagram for model 4 of 85 Peg A with that of a standard solar model having $Y=0.28$ and $Z=0.02$. The theoretical echelle diagram of 85 Peg A has been obtained by using the value of $\Delta = 170\mu\text{Hz}$, and $\nu_0 = 870\mu\text{Hz}$. The lower panel of Fig. 7 obtained for the Sun, is drawn for both the theoretical and the observed frequencies by using the value of $\nu_0 = 690\mu\text{Hz}$ as a reference frequency and a large separation $\Delta = 136\mu\text{Hz}$ corresponding to the observed average which can be calculated on MDI/SOHO frequencies (Schou 1998). Like in the Sun, the theoretical echelle diagram of 85 Peg A shows a regular behaviour of the frequencies, indicating no departures from the simple asymptotic expression. In addition, it is likely that the observed oscillation spectrum of 85 Peg A will not show presence of g modes nor of mixed modes. In fact, our theoretical calculation shows that g modes are well confined in the core and with an amplitude which is too shallow to be detected at the surface. It is important to notice that the observed solar data at high frequencies deviates from the model predictions. This is a consequence of a not fully adequate treatment of the surface layers (see Sec. 6.1). There-

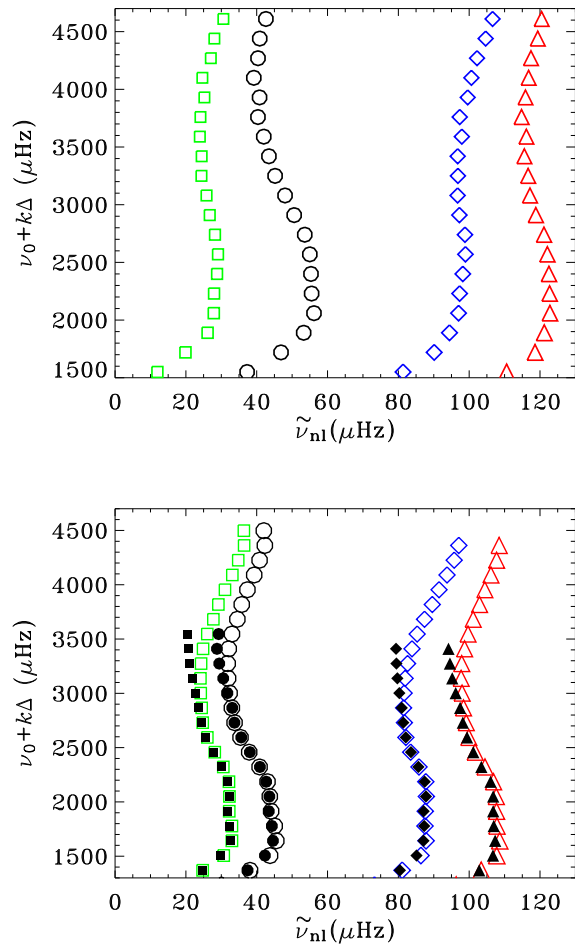


Figure 7. Echelle diagrams respectively for Model 4 (upper panel) of 85 Peg A and a model of the Sun together with the observational results (lower panel). The filled symbols show observed frequencies, while the open symbols represent the computed frequencies. Circles are used for modes with $l=0$, triangles for $l=1$, squares for $l=2$, and diamonds for $l=3$. Theoretical frequencies of 85 Peg A are plotted with $\Delta = 170\mu\text{Hz}$, and $\nu_0 = 870\mu\text{Hz}$. Theoretical and observed frequencies of the Sun are plotted with $\Delta = 136\mu\text{Hz}$ and $\nu_0 = 690\mu\text{Hz}$.

fore this behaviour is also expected for 85 Peg A which is, like the Sun, a low effective temperature star.

8 CONCLUSIONS

In this paper we have addressed the problem of studying the structural properties and identifying the evolutionary state of 85 Peg A. The location in the H-R diagram indicates that this star is in the main-sequence phase of evolution, with a mass in the range $\mathcal{M}=0.75\text{-}0.82\mathcal{M}_{\odot}$ and with an age which can vary from 8 to 14 Gyr. These values have been obtained by assuming the most recent observational parameters of temperature and luminosity, but the classical method of fitting the stellar modeling parameters to the observational data does not allow to reduce the uncertainty on age and mass.

Table 4. Selected models for 85 Peg A obtained with CLES code with and without metal diffusion

mod.	convection	metal diff.	$\mathcal{M}/\mathcal{M}_{\odot}$	$[Z/X]_0$	$[Z/X]_s$	t(Gyr)	L/L $_{\odot}$	R/R $_{\odot}$	T $_{\text{eff}}$	X $_c$
10	MLT	YES	0.788	-0.555	-0.678	11.90	0.615	0.843	5572	0.2035
11	MLT	NO	0.788	-0.555	-0.583	11.96	0.611	0.851	5538	0.2036

Here we have shown that the problem of determining the evolutionary state of 85 Peg A will be solved once observations of the oscillation spectrum will be available for this star. Theoretical calculation of models and p mode oscillations have shown that 85 Peg A is a solar-like star, which is expected to oscillate in the range of frequencies 1000 – 5000 μHz . Our results show that its oscillation spectrum seem to be characterized by a large separation for $l = 0$ of about 150 – 170 μHz and a small separation between $l = 0$ and $l = 2$ which can vary from about 2 to 6 μHz , according to the evolutionary state of the star.

Indeed a difference of about 2 Gyr corresponds, in the asymptotic regime and hence at high frequencies, to a difference in Δ_0 of about 3 μHz and in the ratio d_{02}/Δ_0 of about 0.007 (see Fig. 3). It can be concluded that a determination of frequencies with an uncertainty $\leq 0.8 \mu\text{Hz}$, which corresponds to an average error of ± 0.005 in the ratio d_{02}/Δ_0 , is sufficient to determine the age with an uncertainty better than 2 Gyr.

Our work has examined the role of the most important physical inputs (metallicity, convection and diffusion processes) in the framework of the inputs of our evolutionary code. We have studied the influence of metal diffusion with the help of the CLES evolutionary code, which differs from ours in some physical inputs (e.g. nuclear reaction rates, treatment of helium diffusion, atmospheric boundary conditions, convection modelling). We therefore did not perform an accurate comparison of the codes, but simply have shown that the inclusion of metal diffusion has not an important impact on the age determination. Anyway, the change in metallicity implied by the Thoul et al. (1994) description of metal diffusion is relatively modest ($\sim 33\%$) in 12 Gyr, while FML02 find a reduction of metallicity by more than a factor 2 in ~ 9 Gyr. This difference is taken by us as an indication that really much has to be done in the understanding of this issue.

We believe that this star should be considered as primary target for space or ground-based observations. It is clear indeed that only accurate observations will allow investigation of the properties of the interior of this star and discrimination of its accurate evolutionary stage. The oscillation spectrum of 85 Peg A will reveal how old is the star in terms of core hydrogen consumption, thanks to the very good mass constraint coming from the astrometric and spectroscopic observations. In this respect, it appears feasible to put a lower limit to the age of the Galaxy based on the asteroseismology of 85 Peg A.

ACKNOWLEDGMENTS

The authors are very grateful to G. Houdek for having contributed to the paper with new computations of the amplitude of the oscillations of 85 Peg A. We are also grateful to

the anonymous referee for helpful comments and suggestions which led to the improvement of the present paper. This project has been financially supported by Cofin 2002-2003 "Asteroseismology" through the Italian Ministry of University and Research.

REFERENCES

- Allende Prieto C., Barklem P. S., Lambert D. L., Cunha K., 2004, *A&A*, 420, 183
Alexander D. R., Ferguson J. W., 1994, *ApJ* 437, 879
Angulo C., et al., 1999, *NuPhA*, 656, 3
Basu S., Pinsonneault M. H., & Bahcall J. N., 2000, *ApJ*, 529, 1084
Basu S., Mazumdar A., Antia H. M., Demarque P., 2004, *MNRAS*, 350, 277
Burham S. W., 1879, *Mem RAS*, 44, 141
Böhm-Vitense E., 1958, *Z. Astrophys.* 46, 108
Caloi V., Cardini D., D'Antona F., Badioli M., Emanuele A., Mazzitelli I., 1999, *A&A*, 351, 925
Canuto V. M., Mazzitelli I., 1991, *ApJ* 370, 295
Canuto V. M., Goldman I., Mazzitelli I., 1996, *ApJ* 473, 550
Caughlan, G. R., & Fowler, W. A. 1988, *Atomic Data and Nuclear Data Tables*, 40, 283
Christensen-Dalsgaard J., 1988, in *Advances in Helio - and Asteroseismology*, eds. J. Christensen-Dalsgaard and S. Frandsen, *Proc. IAU Symp.* 123, 295
Christensen-Dalsgaard J., Berthomieu G., 1991, in *Solar Interior and Atmosphere*, eds. A. N. Cox, W. C. Livingston, and M. Matthews Univ. of Arizona Press, *Space Science Series*, Tucson, 401
Fernandes J., Lebreton Y., Baglin A., Morel P., 1998, *A&A*, 338, 455
Fernandes J., Morel P., Lebreton Y., 2002, *A&A*, 392, 529 (FML02)
Flower P. J., 1996, *ApJ*, 469, 355
Fulbright J. P., 2000, *AJ*, 120, 1841
Gratton R. G., et al., 2001, *A&A*, 369, 87
Gratton R. G., Sneden C., Carretta E., 2004, *ARA&A*, 42, 385
Grec G., Fossat E., Pomerantz A., 1983, *Solar Phys.*, 82, 55
Griffin R. F., 2004, *The Observatory*, 124, 258
Hall R. G., 1948, *AJ*, 54, 102
Houdek G., et al. 1999, *A&A*, 351, 582
Iben I. Jr., McDonald J., 1985, *ApJ*, 296, 540
Iglesias C. A., Rogers F. J., 1996, *ApJ* 64, 943
Kjeldsen H., Bedding T. R., 1995, *A&A*, 293, 87
Kjeldsen H., Bedding T. R., 2005, *Proc. SOHO 14/GONG 2004 Workshop*, (ESA SP-559). "Helio - and Asteroseismology: Towards a Golden Future", D. Danesy Ed., p. 101

- Kurucz R. L., 1998, <http://cfaku5.harvard.edu>
- Lippincott S. L., 1981, *PASP*, 93, 376
- Martin C., Mignard F., 1998, *A&A*, 330, 585
- Mazumdar A., Antia H. M., 2001, *A&A*, 377, 192
- Mazzitelli I., 1979, *A&A*, 79, 251
- Mermilliod J.-C., Mermilliod M., Hauck B., 1997, *A&AS*, 124, 349
- Montalbán J., D'Antona F., Mazzitelli I., 2000, *A&A* 360, 935
- Montalbán J., Kupka F., D'Antona F., Schmidt W., 2001, *A&A* 370, 982
- Monteiro M. J. P. F. G., Thompson M. J., 1998, *New Eyes to See Inside the Sun and Stars*, IAU Symp. 185, eds. F.-L. Deubner, J. Christensen-Dalsgaard, D. W. Kurtz, Kluwer, Dordrecht, 317
- Monteiro M. J. P. F. G., Christensen-Dalsgaard J., Thompson M. J., 1994, *A&A*, 283, 247, 1994.
- Monteiro M. J. P. F. G., Christensen-Dalsgaard J., Thompson M. J., 1998, *Ap&SS*, 261, 1
- Monteiro M. J. P. F. G., Christensen-Dalsgaard J., Thompson M. J., 2000, *MNRAS*, 316, 165
- Monteiro M. J. P. F. G., Christensen-Dalsgaard J., Thompson M. J., 2002, *Stellar Structure and Habitable Planet Finding*, 1st Eddington Workshop, eds. F. Favata, I. W. Roxburgh, & D. Galadí-Enríques, ESA-SP 485, 291
- Nordström B., et al. 2004, *A&A*, 418, 989
- Richard O., Michaud G., Richer J., Turcotte S., Turck-Chièze S., VandenBerg D. A., 2002, *ApJ*, 568, 979
- Rogers F. J., Iglesias C. A. 1996, *AAS*, 28, 915
- Rogers F. J., Swenson F. J., Iglesias C. A. 1996, *ApJ*, 456, 902
- Rogers F. J., 2001, *Contributions to Plasma Physics*, 41, 179
- Roxburgh I. W., Vorontsov S. V., 2003, *A&A*, 411, 215
- Roxburgh I. W., 2004, *Second Eddington Workshop: Stellar structure and habitable planet finding*, Eds F. Favata, S. Aigrain, A. Wilson. ESA SP-538, p. 23
- Salaris M., Chieffi A., Straniero O. 1993, *ApJ*, 414, 580
- Saumon D., Chabrier G., van Horn H. M., 1995, *ApJS*, 99, 713
- Schou J. 1998, *Structure and Dynamics of the Interior of the Sun and Sun-like Stars SOHO 6/GONG 98 Workshop Abstract*, Boston, Massachusetts, 6, 47
- Söderhjelm S., 1999, *A&A*, 341, 121
- Stolzmann W., Bloecker T., 1996, *A&A*, 314, 1024
- Stolzmann W., Blöcker T., 2000, *A&A*, 361, 1152
- Struve O., 1955, *stat.conf*, 33
- Tassoul M., 1980, *ApJS*, 43, 469
- ten Brummelaar T., Mason B. D., McAlister H. A., Roberts L. C., Turner N. H., Hartkopf W. I., Bagnuolo W. G., 2000, *AJ*, 119, 2403
- Thévenin F., Idiart T. P., 1999, *ApJ*, 521, 753
- Thoul A. A., Bahcall J. N., Loeb A., 1994, *ApJ*, 421, 828
- Van 't Veer C., 2000, unpublished
- Van't Veer C., Cayrel R., Coupry M. F., Lebreton Y., 2005, *A&A*, in press
- Ventura P., Zeppieri A., Mazzitelli I., D'Antona F., 1998, *A&A*, 334, 953
- Ventura P., D'Antona F., 2005, *A&A*, 431, 279
- Walker G., et al., 2003, *PASP*, 115, 1023